Sunyaev-Zel'dovich signal of the maxBCG SDSS galaxy clusters in WMAP

Patrick Draper, Scott Dodelson, Jiangang Hao, and Eduardo Rozo

Phys. Rev. D **85**, 023005 — Published 18 January 2012

DOI: 10.1103/PhysRevD.85.023005

The Sunyaev-Zeldovich Signal of the maxBCG SDSS Galaxy Clusters in WMAP

Patrick Draper[1,5], Scott Dodelson[2,3,4], Jiangang Hao[2], Eduardo Rozo[3,4]
[1]*Enrico Fermi Institute, The University of Chicago, Chicago, IL 60637*
[2]*Center for Particle Astrophysics, Fermi National Accelerator Laboratory, Batavia, IL 60510*
[3]*Department of Astronomy & Astrophysics, The University of Chicago, Chicago, IL 60637*
[4]*Kavli Institute for Cosmological Physics, Chicago, IL 60637 and*
[5]*Santa Cruz Institute for Particle Physics, Santa Cruz, CA 95064*

The Planck Collaboration measured the Sunyaev-Zel'dovich (SZ) decrement of optically selected clusters from the Sloan Digital Sky Survey, finding that it falls significantly below expectations based on existing mass calibration of the maxBCG galaxy clusters. Resolving this tension requires either the data to go up, or the theoretical expectations to come down. Here, we use data from the Wilkinson Microwave Anisotropy Probe (WMAP) to perform an independent estimate of the SZ decrement of maxBCG clusters. The recovered signal is consistent with that obtained using Planck, though with larger error bars due to WMAP's larger beam size and smaller frequency range. Nevertheless, this detection serves as an independent confirmation of the magnitude of the effect, and demonstrates that the observed discrepancy must originate in modeling or other systematic uncertainties.

Introduction. Galaxy clusters are the largest gravitationally bound objects in the Universe and potentially powerful probes of dark matter and dark energy. Understanding clusters well enough to use them as probes requires a multi-wavelength approach, as observations from the radio to the gamma ray end of the spectrum reveal different features of clusters. Observations of the cosmic microwave background (CMB) can detect the Sunyaev-Zel'dovich (SZ) effect [3, 4, 10], wherein hot electrons distort the spectrum of passing photons. The distortion has a characteristic spectral shape and the morphology of the signal traces the integrated pressure of the cluster.

The SZ effect was first detected with high resolution and sensitivity measurements of individual clusters, and these have become so powerful that hundreds of clusters are expected to be detected by telescopes such as the South Pole Telescope (SPT) [11] and Atacama Cosmology Telescope (ACT) [7–9]. However, with large galaxy surveys such as the Sloan Digital Sky Survey (SDSS), which detect tens of thousands of clusters optically, even relatively low resolution CMB surveys such as WMAP [5] can detect the SZ signal by stacking many clusters with the same optical properties.

Recently, the Planck Collaboration [1] performed such a measurement utilizing the SDSS maxBCG cluster catalog [12]. This catalog has been used to place tight cosmological constraints on the amplitude of matter fluctuations [19] that are consistent with those derived from X-ray selected cluster catalogs [21–23]. Moreover, the corresponding cluster mass estimates from Johnston et al. [14] — modified as per Rozo et al. [20] — are consistent with the X-ray luminosity as estimated in [18], and velocity dispersion measurements as estimated by [15]. Surprisingly, the Planck Collaboration [1] found that the SZ-decrement from these clusters fell significantly below their expectations. If real, this discrepancy signals that either some aspect of the physics of the intra-cluster medium is not properly understood, that the selection of optically selected clusters is not adequately understood despite the successes it has enjoyed thus far, or that there is a hidden systematic in the data[1] We note too that this discrepancy may not the same as that discussed in other works that compare the predicted and observed SZ signal of X-ray selected clusters (e.g. [6, 25–27], though see also [28, 29]), as [30] explicitly checked that their SZ estimates are in fact consistent with expectations from X-ray.

Here we attempt to confirm the Planck measurement by searching for the SZ signal in WMAP caused by the SDSS maxBCG galaxy clusters. We analyze the data using both parametric and non-parametric techniques. In both cases, we detect

[1] One plausible candidate might be contamination from radio sources. However, [6] estimate that for massive galaxy clusters, point source contamination is $\approx 5\%$, much too small to be of relevance for our analysis. We have verified that using the source excess counts from Coble et al. [16] with the de Zotti et al. [31] model results in a similar estimate for the point source contamination of the richest systems. Assuming radio source counts scale with richness, the expected contamination for our lowest richness systems is $\approx 20\%$. This appears large, but has to be compared to our estimated error $\approx 80\%$ for the same bin. Overall, the quality of the data is such that point source contamination is not expected to be significant.

a signal that increases with cluster richness, with an amplitude consistent with that observed by Planck [1]. Throughout this work, we adopt a fiducial flat ΛCDM cosmology with $\Omega_m = 0.3$ and $h = 0.7$. Cluster masses are defined within a radius R_{500} such that the overdensity is 500 times that of the critical density of the universe.

Data. From the WMAP single-year, foreground-reduced, W-band, high-resolution ($N_{side} = 1024$) temperature fluctuation maps, we take the noise-weighted mean to construct 7-year coadded maps. For each year, we subtract off an overall map mean found from the noise-weighted average of 10^6 random, unique, unmasked Healpix pixels containing no MaxBCG clusters and removing outliers. The resulting map contains the temperature and noise in 12.6 million $(3.4')^2$ pixels.

We use the WMAP maps to estimate the SZ signal of maxBCG galaxy clusters [12]. The catalog is constructed by searching for red-sequence galaxies drawn from the SDSS Data Release 5, and includes 13,823 galaxy clusters over 7500 deg^2 in a redshift slice $z \in [0.1, 0.3]$. Each cluster is assigned a richness N_{200}, the number of galaxies within 2σ of the red-sequence and within a specified radial aperture [see 12, for details]. Cluster redshifts are photometrically estimated and are accurate at the $\Delta z \lesssim 0.01$ level. The input for our analysis is the position angle (RA, DEC), redshift (z), and richness (N_{200}) of each cluster.

Analysis. The SZ signal at angular position $\vec{\theta}$ relative to a cluster center is an integral of the electron pressure P along the line of sight:

$$\frac{\Delta T_{\rm SZ}(\vec{\theta};\nu)}{T} = \frac{\sigma_T g(\nu)}{m_e c^2} \int_{-\infty}^{\infty} dl P\left(\vec{x}[\vec{\theta}, d_A(z), l]\right), \quad (1)$$

where g is the characteristic spectral shape of the SZ distortion equal to -2 at very low frequencies, σ_T is the Thomson cross section, and — with the cluster centered at the origin — the 3D position $\vec{x}$ has components equal to $(d_A(z)\vec{\theta}, l)$, where $d_A(z)$ is the angular diameter distance out to the redshift of the cluster.

We employ two complementary techniques to extract the weak SZ signal from the WMAP data: a parametric and a non-parametric approach. In the parametric ("matched filter") approach, we take as input the data $d_i = \Delta T_i$ in pixels around each cluster, the covariance matrix C_{ij} connecting the pixels (which includes both instrumental noise and correlations due to the primordial CMB), and a morphological template t_i for the signal in each pixel. We then minimize χ^2 with

$$\chi^2(A) = \sum_{i=1}^{N_{\rm pixels}} (d_i - A t_i)\, C_{ij}^{-1}\, (d_j - A t_j)$$

N_{200} bins ($\langle N \rangle$)	Cluster Count	M_{500} ($10^{13} M_\odot$)	θ_{500} (arcmin)	$\tilde{Y}_{500} \times 10^4$ (arcmin^2)
8-30 (14)	12408	8.5	3.2	$0.35 \pm .27$
31-50 (37)	690	24	4.5	2.9 ± 1.5
51-80 (60)	160	40	5.3	4.9 ± 3.2
81-200 (104)	33	71	6.4	21 ± 6.8

TABLE I. Properties of the four bins in N_{200}. The number of clusters is taken after the WMAP mask is applied, and the mean number in each bin is used to calculate M_{500} and θ_{500} for a redshift $z = 0.2$. The SZ measurement is given in the final column. The errors are estimated from the filter noise.

where A is the dimensionless amplitude of the signal. The sum is over all $N_{\rm pixels}$ within an angular radius $\theta_{max} = 5 \times \theta_{500}$ of the cluster center, where $\theta_{500} = R_{500}/d_A(z)$. The estimate of R_{500} requires a mass-richness relation, which we take to be ([20])

$$\langle M_{500}|N_{200}\rangle = e^{B_{M|N}} \left(\frac{N_{200}}{40}\right)^{\alpha_{M|N}} \times 10^{14} M_\odot,$$

with $B_{M|N} = 0.95 \pm 0.12$ and $\alpha_{M|N} = 1.06 \pm 0.11$. Table I lists the richness bins in N_{200}, the assumed masses, and the angular extent of the clusters at $z = 0.2$.

To obtain the elements of the covariance matrix, we first compute the beam-convolved CMB correlation function $\xi(\theta)$ using the C_l corresponding to WMAP7 parameters [6]. For each pair of pixels i, j we determine the angular separation $\theta_{ij} \equiv [\theta_i^2 + \theta_j^2 - 2\theta_i\theta_j \cos(\phi_i - \phi_j)]^{1/2}$ between the centers of the pixels, and set the element of the covariance matrix $C_{ij} = \xi(\theta_{ij})$. The full covariance matrix is set by adding the diagonal noise contribution $N_i^2 \delta_{ij}$. For the template, we choose the pressure profile in Arnaud et al. [2]:

$$P(r) = 1.65\,{\rm eV\,cm^{-3}} E^{8/3}(z) \times \left[\frac{\langle M_{500}|N_{200}\rangle}{3 \times 10^{14} M_\odot}\right]^{0.79} p(r/R_{500}), \quad (2)$$

where $p(x)$ is the dimensionless profile

$$p(x) \equiv \frac{8.403}{(c_{500}x)^\gamma [1 + (c_{500}x)^\alpha]^\delta}$$

with $c_{500} = 1.177, \alpha = 1.051, \gamma = 0.3081$, and $\delta = 4.931$. The predicted signal in a pixel i is $\Delta T_{\rm SZ}$ as computed from Eq. (1), convolved with the WMAP beam $B(\vec{\theta} - \vec{\theta}_i)$:

$$t_i = \int d^2\theta\, B(\vec{\theta} - \vec{\theta}_i)\, \Delta T_{\rm SZ}(\vec{\theta}).$$

Minimization of the χ^2 for a given cluster α leads to an estimate of the amplitude:

$$\hat{A}_\alpha = \sum_{ij} \sigma^2_{A,\alpha} t_i C^{-1}_{ij} d_j$$

with "filter noise" (the error due solely to instrument noise+CMB) defined as

$$\sigma^{-2}_{A,\alpha} = \sum_{ij} t_i C^{-1}_{ij} t_j.$$

An amplitude estimate $\hat{A}_\alpha = 1$ corresponds to data that is exactly consistent with the assumed template. The mean amplitude $\langle \hat{A} \rangle$ for a richness bin is defined as the inverse-variance weighted average of $\hat{A}_\alpha$ over all clusters in the bin. Due to intrinsic scatter in the mass-richness relation, the total error on $\hat{A}$ will be larger than the filter noise. Therefore, we inverse-variance weight the amplitudes by the total error, defined as the sum in quadrature of the filter error and the intrinsic scatter. To estimate the intrinsic scatter, we compute the scatter in a given richness bin,

$$\sigma^2_{\langle A \rangle, total} = \frac{1}{N(N-1)} \sum_{i=1}^{N} (\hat{A}_i - \langle \hat{A} \rangle)^2$$

and then subtract $\sigma^2_{\langle A \rangle, filter}$. Since the weighting depends on the total error, we iterate until the input total error is equal to the output scatter.

The template and the measured value for the amplitude A can be transformed into an estimate of any related quantity. One relevant quantity is $\tilde{Y}_{500}$, defined as

$$\tilde{Y}_{500} \equiv \frac{\sigma_T}{m_e d_A^2} E^{-2/3}(z) \left(\frac{d_A(z)}{500\,\mathrm{Mpc}} \right)^2 \int d^3 r P(\vec{r})$$

where the integral is restricted to $r < R_{500}$. Using the template in Eq. (2), we find

$$\tilde{Y}_{500} = 8.5 \times 10^{-4} A \left(\frac{\langle M_{500} | N_{200} \rangle}{3 \times 10^{14} M_\odot} \right)^{1.79} \mathrm{arcmin}^2.$$

We also carry out a non-parametric fit by averaging the temperatures in pixels binned into annuli around the clusters. As in the matched filter approach, the covariance matrix for the annuli-averaged temperatures contains contributions from instrument noise and from the primordial CMB. The first is straightforward to propagate using the combined weights from the single year WMAP maps. To compute the second, we first note that the estimated temperature in a given annulus a distance θ from a given point, taken to be the origin, is $T_\theta = \frac{1}{N} \sum_{i=1}^{N} T(\theta, \phi_i)$,where the sum is over all N pixels in the annulus, each identified by its polar position ϕ_i. The covariance matrix between measurements in two annuli at θ and θ' is

$$C_{\theta\theta'} = \frac{1}{NN'} \sum_{i=1}^{N} \sum_{i'=1}^{N'} \langle T(\theta, \phi_i) T(\theta', \phi'_{i'}) \rangle.$$

Here N' is generally not equal to N since larger annuli have more pixels (of fixed size) in them. The average of the product of the temperatures is $\xi(\theta_{ii'})$, the correlation of the CMB between two pixels separated by angular distance $\theta_{ii'}$.

We use 11 annuli with angular distance from the cluster equal to $(0.5, 0.9, 1.3, \ldots, 4.5) \times \theta_{500}$. The CMB noise is the same order of magnitude as the instrumental noise but is highly correlated between rings, so a simple χ-by-eye of the profile is not sufficient to interpret the results. We ran 100 mocks to test this approach and found that the extracted amplitude A is biased high by 1.35 ± 0.25 for the $51-80$ richness bin and 1.67 ± 0.62 for the top bin. We correct for these biases below.

Results. Fig. 1 shows our estimates for $\tilde{Y}_{500}$ for clusters in the four richness bins. The corresponding amplitudes are $\hat{A} = 0.40 \pm 0.30, 0.52 \pm 0.27, 0.35 \pm 0.24, 0.53 \pm 0.17$. The error bars are $\sigma_{\langle A \rangle, filter}$ propagated from $\hat{A}$ to $\tilde{Y}_{500}$. We also estimate the total scatter with $\sigma_{\langle A \rangle, total}$, which is sensitive to outlier clipping. In Table II we give values for $\sigma_{\langle A \rangle, filter}$ and $\sigma_{\langle A \rangle, total}$ without clipping, and compute the contribution from intrinsic scatter.

Our measurements are in excellent agreement with those of the Planck Collaboration [1], and

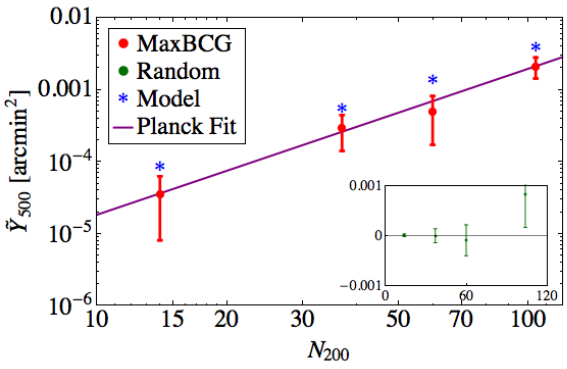

FIG. 1. W band SZ signal in 4 N_{200} bins. The blue stars show the expectation for the SZ decrement of the maxBCG clusters based on the Rozo et al. (2009) mass-richness relation, while the red circles show the signal measured using WMAP data. The error bars are set by the filter noise. The solid line shows the best-fit result from Planck. The inset shows that randomizing the positions of the clusters within the survey area leads to a signal consistent with zero.

$\langle N_{200}\rangle$	$\sigma_{\langle A\rangle,total}$	$\sigma_{\langle A\rangle,filter}$	$\sigma_{\langle A\rangle,intrinsic}$
14	0.68	0.27	0.62
37	2.2	1.5	1.6
60	5.3	3.2	4.2
104	13	6.8	11

TABLE II. Mean $\tilde{Y}_{500}$ errors in units of 10^{-4} arcmin^2. The filter noise includes only uncertainties from the instrument and the CMB. The quadrature difference between the total dispersion and the filter noise gives an estimate for the error in the mean due to intrinsic scatter.

are clearly lower than the theoretical predictions. Given this independent confirmation of the tension first observed in [1], it is clear that either the intra-cluster properties of galaxy clusters are not adequately understood, or that the optical cluster selection suffers from a systematic that has gone undetected. We do not currently know the solution to this problem, and indeed, the discrepancy is likely to remain an active field of research in the immediate future. We note that a similar discrepancy appears to arise for the SZ signal about Luminous Red Galaxies (LRGs) [24].

We perform three systematics cross-checks of our analysis pipeline: first, we randomize the location of every cluster in the catalog and repeat our measurement. As expected, we find no signal. In addition, we generate Monte Carlo realizations of the experiment to test whether the recovered amplitude is biased. We randomly sample the maxBCG catalog, and assign to every cluster an SZ decrement (including scatter, for which we vary $\sigma_{\ln Y}$ from 0.6 to 1.2). The cluster signal of Eq. (1) is convolved with the beam and added to randomly generated (beam-convolved) CMB maps. We then fit for the amplitude of the signal using our pipeline, finding that the recovered signal is biased low by 2% (3%) in the $51-80$ bin and 5% (6%) in the $81-200$ bin for $\sigma_{\ln Y} = 0.6$ (1.2). Finally, we test for biases due to cluster-cluster correlations, caused by the presence of large scale structure. This test is similar to the previous, using random global rotations of the WMAP maps instead of random maps. We do not detect additional bias in the recovered signal.

Fig. 2 shows the non-parametric measurement for the signal as a function of distance from the cluster center in the two largest richness bins. A simple χ^2 assuming no signal reveals strong detections in both bins ($\chi^2 = 23.1, 25.6$ for 10 degrees of freedom each). The smooth curves show the predicted signal from our fiducial template template ($A = 1$). The best fit for the two bins

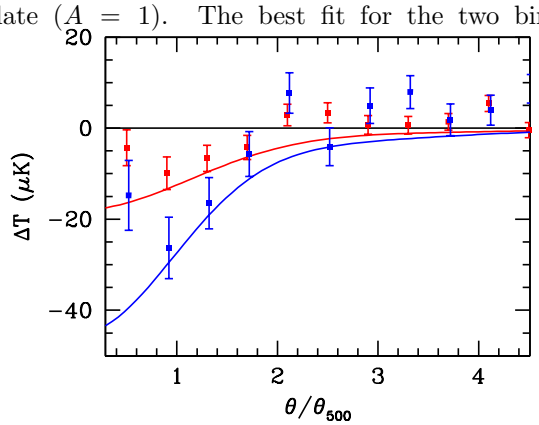

FIG. 2. W band SZ signal as a function of distance from the cluster center for clusters in the second-largest (red) and largest (blue) richness bins listed in Table 1. Error bars include instrumental noise only. Solid curves are the predictions from the template assumed in Eq. (2). The deviation on small angular scales translates into a smaller amplitude than assumed, in agreement with the Planck results.

yields $A = 0.76 \pm 0.24$ for the $N_{gals} = 51-80$ bin and $A = 0.77 \pm 0.22$ for the highest richness bin ($\chi^2 = 13.3, 13.5$ for 10 degrees of freedom each). Correcting for the 35% and 67% biases discussed previously in these bins leads to estimates of $A = 0.56$ and 0.46 respectively, consistent within errors with the parametric determination. The latter is the superior way to determine the amplitude as it weights all pixels optimally, albeit at the cost of being sensitive to the assumed template.

ACKNOWLEDGMENTS

SD and JH are supported by the US Department of Energy, including grant DE-FG02-95ER40896; and SD by National Science Foundation Grant AST- 0908072. ER is funded by NASA through the Einstein Fellowship Program, grant PF9- 00068.

[1] N. Aghanim *et al.* [Planck Collaboration], arXiv:1101.2027.
[2] M. Arnaud *et al.* 2009 arXiv:0910.1234.
[3] Birkinshaw, M. 1999, Phys. Reports, 310, 97
[4] Carlstrom, J. E., Holder, G. P., & Reese, E. D. 2002, Ann.Rev.Ast.Astrophy., 40, 643
[5] N. Jarosik *et al.*, Astrophys. J. Suppl. **192**, 14 (2011).

[6] E. Komatsu *et al.* [WMAP Collaboration], Astrophys. J. Suppl. **192**, 18 (2011).
[7] Sehgal, N., et al. 2011, Astrophys. J., 732, 44
[8] Marriage, T. A., et al. 2010, arXiv:1010.1065
[9] F. Menanteau *et al.*, Astrophys. J. **723**, 1523 (2010).
[10] Sunyaev, R. A. & Zeldovich, Y. B. 1972, Comments on Astrophysics and Space Physics, 4, 173
[11] K. Vanderlinde *et al.*, Astrophys. J. **722**, 1180 (2010)
[12] Koester, B. P. *et al.* 2007, Astrophys. J., 660, 239
[13] Sheldon, E. S. *et al.* 2009, Astrophys. J., 703, 2217
[14] Johnston, D. E. *et al.* 2007, arXiv:0709.1159
[15] Becker, M. R. *et al.* 2007, Astrophys. J., 669, 905
[16] Coble, K. *et al.* 2007, Astron. J. **134**, 897-905.
[17] Gralla, M. B. *et al.* 2011, Astrophys. J., 737, 74.
[18] Rykoff, E. S. *et al.* 2008, Astrophys. J., 675, 1106
[19] Rozo, E. *et al.* 2010, Astrophys. J., 708, 645.
[20] Rozo, E. *et al.* 2009, Astrophys. J., 699, 768.
[21] Mantz, A. *et al.* 2010, MNRAS, 406, 1759.
[22] Vikhlinin, A. *et al.* 2009, Astrophys. J., 692, 1060.
[23] Henry, J. P. *et al.* 2009, Astrophys. J., 691, 1307.
[24] Hand, N. *et al.* 2011, arXiv:1101.1951.
[25] Lieu, R. *et al.* 2006, Astrophys. J., 648, 176.
[26] Bielby, R.M. and Shanks, T. 2007, MNRAS, 382, 1196.
[27] Diego, J.M. and Partridge, B. 2010, MNRAS, 402, 1179.
[28] Afshordi, N. *et al.* 2007, MNRAS, 378, 293.
[29] Melin, J.B. *et al.* 2011, A&A, 525, 139.
[30] Planck Collaboration, arXiv:1101.2043.
[31] de Zotti, G. *et al.* 2005, A&A, 431, 893.